Modelling and experimental validation of Textile Pockets based active inflatable device

A. Mehmood *§, M. Basset *, R. Orjuela *, R. Dupuis *, J. Y. Drean †
* MIPS laboratory (EA 3223), University of Haute-Alsace
12 rue des frères lumière F-68093, Mulhouse, France.
†LPMT laboratory (EA 4365), University of Haute-Alsace
11 rue Alfred Werner F-68093 Mulhouse, France.
§COMSATS Institute of Information Technology,
Park road Islamabad, Pakistan.

Abstract

This paper aims with the mathematical modelling of an active inflatable device. This device is composed of a compressor, an Electro-pneumatic Pressure Converter (EPC) and an Inflatable Textile fabric Pocket (ITP). The later has interesting mechanical properties and is fabricated using Jacquard knitting technique which allows automatic production of unlimited varieties of pattern weaving without any mould. Thanks to these features, these ITPs have provided a better alternative to the classical airbags made by stretchable polymer material. The proposed mathematical model is obtained by combining sub-models of two main parts of the whole system. In this way, a generalized and flexible model is obtained which can easily take into consideration the ITPs of different shapes. The pressure dynamics inside the ITP are considered by taking into account the air flow rate, variation of the volume of ITP and the length of pneumatic lines joining ITP with compressed air source. The parameters of the whole mathematical model are obtained via identification techniques. The effectiveness of the model is assessed through several experimental tests with the help of a servo hydraulic fatigue testing machine.

Keywords: Electro-pneumatic Pressure Converter, Inflatable Textile Pocket (ITP), Modelling

Nomenclature

F	Force	A	Area
V	Volume	R	Air gas constant
ν	Poisson ratio of chamber	p	Pressure
T	Temperature	γ	Specific heat ratio
ρ	Density	u	Applied voltage signal
m	Mass	$\dot{m}$	Mass flow rate
d	Damping coefficient	k	Spring coefficient
s	Thickness of chamber	E	Young modulus of chamber
m_v	Pocket mass	σ	Stress of chamber
r	Radius of spherical chamber	a	Semi-major axis of elliptical chamber
b	Semi-minor axis of elliptical chamber	c	Width of elliptical chamber
ε	Deformation of chamber	R_t	tube resistance
v_a	velocity of air	v_c	velocity of sound

Subscript and abbreviation

$s-out$	Pocket outward direction	in	Initial	fin	Final
$s-in$	Pocket inward direction	p	Plunger	s	Pocket
res	Reservoir	atm	Atmospheric	ext	External
$down$	Downstream	up	Upstream	mag	Magnet force
θ	Circumferential / hoop	a	Longitudinal		

1 Introduction

The active inflatable devices have many interesting industrial applications. In the automotive industry for example, the inflatable devices are widely used to improve driver's safety e.g. steering airbags, inflatable bumpers and inflatable seat belts [1, 2]. Recently, active inflatable devices are also employed in the car seats to replace polyurethane foam improv-

ing in this way driver's comfort and safety [3, 4]. In fact, polyurethane foam provides interesting mechanical properties, low density, capacity to absorb energy and low stiffness. However, polyurethane material degrades in quality and becomes denser over time and consequently less comfortable for the drivers. Furthermore, the recycling process of polyurethane foam is also difficult. Nowadays, the employed inflatable pockets are made with stretchable polymer material which may be easily torn off. Moreover, these components are made by molds which means that each design requires a separate mold. Currently researchers are looking for solutions to replace classical stretchable polymer materials by smart textile [5, 6].

In the proposed active inflatable device, classic inflatable material is replaced by new Inflatable Textile Pockets (ITP) that are fabricated on 3D fabric weaving machines. Considering the state-of-the-art 3D fabric designs are conceived as a productive insight in terms of both weight and cost [7]. Mostly, two distinct sets of yarns or threads are interlaced at right angles to form a fabric or cloth in 2D. However, to create the third dimension, additional warp yarns are manipulated to obtain a 3D fabric. In this paper, the employed ITPs are fabricated using Jacquard knitting technique which allows automatic production of unlimited varieties of pattern weaving without any mould. Some recent studies have shown that these ITPs are not only better than classical materials with respect to strength but offers computer aided designing of different complex and inflatable structures [8, 6].

This contribution presents a first issue of a new active inflatable device using Inflatable Textile Pocket technology. The paper is mainly focused on the mathematical modelling and experimental validation of an inflatable device composed of a pressure supply, an Electro-pneumatic Pressure Converter (EPC) and an Inflatable Textile Pocket. Until now, modelling and experimental validation of an ITP-based inflatable device have not been proposed in the literature to the best of authors' knowledge. The proposed structured mathematical model will be further extended to a model based control of a more complex active system in the later stages.

The proposed ITP based system is pressurized through a pressure converter with a proportional servo valve, i.e. a pressure converter (EPC), in order to regulate the pressure inside it. Since the EPC is an important part of ITP device, it has a significant impact on pressure dynamics. It consists of a plunger which may attain different positions linearly proportional to the applied signal (see for example [9] and [10]). Modelling of the proportional valve considered in this study has already been discussed for the application of servo pneumatic actuators in the literature [11, 12, 13, 14]. However, dynamic behaviour of the EPC changes with each mark and application. Furthermore, its application to pressurize an inflatable device was not addressed to the best of authors' knowledge. Therefore, the spool valve dynamics are considered here, for dynamic analysis of pressure. The spring action on the solenoid based spool valve allows it to attain different pressure values inside the ITP.

The pressure inside the ITP depends on flow of air through the EPC, modelled by using orifice flow equations [15] and pneumatic lines dimensions [16]. The fabric material, in terms of forces and deformations, has been characterized to determine the evolution of the pocket volume. Besides, the rigidity of the pocket is equally important to be taken into consideration for the pressure distribution [17]. Therefore, the pocket strength has also been observed carefully at various pressures. Finally, the mathematical model of the whole inflatable device, proposed here, is based on two sub-systems i.e. the EPC and the ITP. Each sub-system can be modelled independently to ensure a flexible and generalized model of the system: for example, a model that takes ITPs with different shapes into consideration. A test bench is employed to assess the abilities of the proposed model. Several tests are performed which affirm the effectiveness of the proposed model.

This article is organized as follows: In Section 2 the modelling of the inflatable device is proposed. The Electro-pneumatic Pressure Converter (EPC) is described by considering it as a bi-directional spool valve. The air bag dynamics are also studied in this section by considering two ITP shapes i.e. spherical and elliptical shapes. Then, the developed models of these two ITPs are also presented. Finally, pressure variation inside the ITP is considered by taking into account the mass flow dynamics, pressure loses in pneumatic

lines and variation in the volume of ITP. In Section 3, different parameters of the model are identified using the least square method. The developed model with the identified parameters is validated in Section 4. Last but not the least, Section 5 concludes the article.

2 ITP System modelling

Here, the whole active inflatable device consists of a compressor, the Electro-pneumatic Pressure Converter (EPC) and an Inflatable Textile Pocket (ITP). An interesting use case of this inflatable device, considered here, is an active seat cushion shown in Fig.1. Each ITP can sustain an absolute pressure up to $2Bar$ as presented in [6]. The EPC is a proportional servo valve which regulates the pressure inside the inflatable device. In this section, modelling of the two main parts of the system i.e. the pressure converter and the inflatable textile pocket is discussed. The impact of pneumatic lines joining all sub parts of the inflatable device is considered by modelling the air flow with one dimensional wave equations. Notice that the mathematical model can be easily modified by taking into account different shaped pockets and length of pneumatic lines. In this paper, for example, two shaped pockets are investigated.

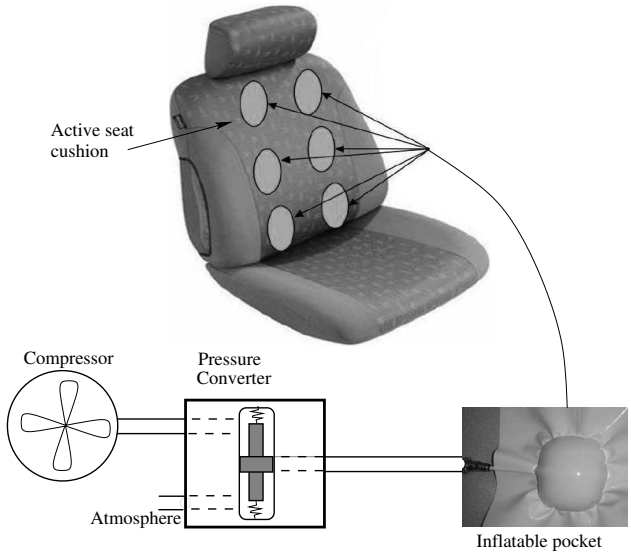

Figure 1: An active inflatable device composed of Inflatable Textile Pockets

2.1 Electro-pneumatic pressure converter (EPC) modelling

The EPC is a five port three positions valve with closed center. It has a built-in electronic circuit which allows pressure variation at the outlet port. The supply port is connected to a pressure reservoir while the output port is connected to the ITP. The generated electromagnetic force induces linear movement of the plunger when the solenoid coils are energized. The principle of the 5/3 (five ports 3 positions closed center) proportional spool valve is shown in Fig.2.

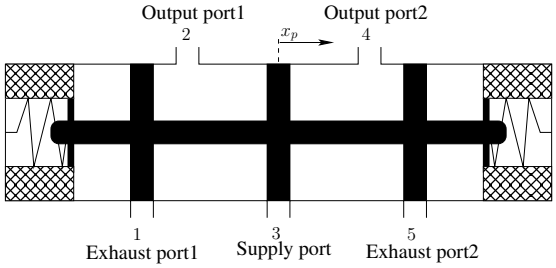

Figure 2: Schematic diagram of a 5/3 proportional spool valve at its closed center position

In order to model it, the mechanical equation of the spool valve is obtained from Newton's second law considering all the important forces acting on it and given as follows:

$$m_p \ddot{x}_p = F_{mag} - (p_s - p_{atm})\, A_p - d_p \dot{x}_p - k_p x_p \tag{1}$$

where m_p, x_p, d_p and k_p are respectively, the plunger mass, the plunger position, its damping constant and spring constant. A_p and p_s are, respectively, the spool valve area and the pressure inside the pocket. As proposed in [18] the magnetic force F_{mag} can be characterized by the following equation:

$$F_{mag} = Du(t - \tau) \tag{2}$$

where D is a constant value in VN^{-1} and τ represents the delay in the applied voltage signal u. Since, this delay is caused by the integrated electronic circuit of the valve, therefore its physical model is very difficult to determine. Hence, it is identified experimentally as a function of the applied voltage (see Table.2). The proposed model of the EPC in the state

space form is, then, summarized here after:

$$\dot{x}_1 = x_2 \tag{3a}$$

$$\dot{x}_2 = -\left(\left(p_s - p_{atm}\right) A_p + d_p x_2 + k_p x_1\right)/m_p + \left(D/m_p\right) u(t-\tau) \tag{3b}$$

where x_1 and x_2 are, respectively, the position and the velocity of the plunger. In the next part, the pressure dynamics inside the ITP is described by considering the air flow dynamics and the variation in the pocket volume.

2.2 Pressure inside the ITP

The pressure inside the pocket is modelled by using ideal gas equation. Here, the variation in temperature of the gas is neglected and consequently the following equation is obtained [15]:

$$p_s V_s = m_s R T_s \tag{4}$$

where p_s, V_s, m_s, R and T_s are respectively, the pressure inside the pocket, its volume, the amount of air mass inside it, the gas constant for air and the temperature inside. The pressure inside the ITP depends on its volume and flow of air into the pocket. Therefore, by taking the partial derivative of equation (4) we get:

$$\dot{p}_s = \frac{R T_s}{V_s}\dot{m}_s - \frac{p_s}{V_s}\dot{V}_s \tag{5}$$

2.2.1 Air mass flow

The air mass flow through a duct can be represented as a Barré de Saint-Venant equation used for compressible fluid flow [19]. Indeed, the orifice of the proportional valve is considered as a duct [15]. The air can flow either from the ITP to atmosphere or from air pressure source to the ITP. Pneumatic lines joining the ITP to the atmosphere or the pressure source may attenuate the air flow due to pneumatic line resistance. This aspect has also been considered while modelling the ITP, because long pneumatic lines cause the drop in air pressure and delay in air flow [20]. The total amount of air mass flow to the pocket is the difference of air flowing in and out from it, which is expressed as follows:

$$\dot{m}_s = \dot{m}_{s-in} - \dot{m}_{s-out} \tag{6}$$

The equation of air flow from ITP towards atmosphere $\dot{m}_{s-out}$ is given by the following equation [19]:

$$\dot{m}_{s-out} = A_{eff(s-atm)} p_s \sqrt{\frac{\gamma}{RT_s}} \Phi\left(p_r\right), \quad \text{with} \quad p_r = \frac{p_s}{p_{atm}} \tag{7}$$

where $A_{eff(s-atm)}$ is the effective flow area between the pocket and the atmosphere. The function $\Phi(p_r)$ is an expression which depends on the upstream and the downstream pressure ratio p_r. Here, the upstream pressure is the pressure in the ITP (p_s) and the downstream pressure is the atmospheric pressure (p_{atm}). Similarly, the flow of air from source reservoir considered as an infinite source of pressure to the pocket $\dot{m}_{s-in}$ is represented by:

$$\dot{m}_{s-in} = A_{eff(res-s)} p_{res} \sqrt{\frac{\gamma}{RT_{res}}} \Phi\left(p_r^*\right), \quad \text{with} \quad p_r^* = \frac{p_{res}}{p_s} \tag{8}$$

here, $A_{eff(res-s)}$ is the effective flow area of the valve between the pocket and the source reservoir. In this case, the upstream pressure is the pressure of the source (p_{res}) and the downstream pressure is the pressure in the ITP (p_s). The pressure ratio p_r in equation (7) depends upon the amount of fluid mass which causes an increase in downstream pressure or drop in upstream pressure. When this ratio is less than or equal to 0.528, the fluid flow enters to subsonic or supersonic conditions [15, 19], and the amount of air flow becomes constant. The expression for subsonic and supersonic conditions is given by [15]:

$$\Phi\left(p_r\right) = \begin{cases} \sqrt{\left\{\left(p_r\right)^{2/\gamma} - \left(p_r\right)^{(\gamma+1)/\gamma}\right\} \frac{2}{\gamma-1}}, & p_r \geq \left(\frac{2}{\gamma+1}\right)^{\gamma/(\gamma-1)} \\ \sqrt{\left(\frac{2}{\gamma+1}\right)^{(\gamma+1)/2(\gamma-1)}} & , \; p_r < \left(\frac{2}{\gamma+1}\right)^{\gamma/(\gamma-1)} \end{cases} \tag{9}$$

where γ is specific heat ratio for air. The tube connecting the EPC with the pneumatic actuator may have two impacts on the flow. First, the pressure drop because of tube resistance and second, the delay in the flow due to the wave travel time through the long tube. Fig. 3 shows one dimensional air flow through a pneumatic pipe of length L_l and cross section A_l. Based on the mass, continuity and equilibrium equations for one dimensional flow, the basic differential equations governing transient flow in a tube are given below (see [21]):

$$\frac{\partial v_a}{\partial x_l} = -\frac{1}{\rho v_c^2} \frac{\partial p}{\partial t} \tag{10a}$$

$$\frac{\partial p}{\partial x_l} = -R_t v_a - \rho \frac{\partial v_a}{\partial t} \tag{10b}$$

where R_t, v_a and v_c are, respectively, the tube resistance, the velocity of air and the velocity of sound.

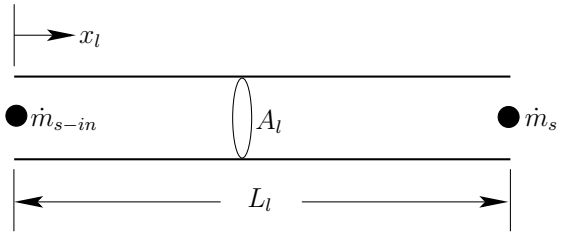

Figure 3: The air mass flow through pneumatic tube line

Replacing the velocity of air by introducing the air mass flow equation $\dot{m} = \rho A_l v_a$ which represents the air flow through a tube of same cross sectional area into (10a) and (10b) gives:

$$\frac{\partial \dot{m}}{\partial x_l} = -\frac{A_l}{v_c^2}\frac{\partial p}{\partial t} \tag{11a}$$

$$\frac{\partial p}{\partial x_l} = -\frac{R_t \dot{m}}{\rho A_l} - \frac{1}{A_l}\frac{\partial \dot{m}}{\partial t} \tag{11b}$$

where ρ and A_l are the air density and the cross sectional area of tube. Now, the partial derivative of equation (11a) with respect to x_l and the partial derivative of equation (11b) with respect to t are given by:

$$\frac{\partial^2 \dot{m}}{\partial x_l^2} = -\frac{A_l}{v_c^2}\frac{\partial^2 p}{\partial x_l \partial t} \tag{12a}$$

$$\frac{\partial^2 p}{\partial x_l \partial t} = -\frac{R_t}{\rho A_l}\frac{\partial \dot{m}}{\partial t} - \frac{1}{A_l}\frac{\partial^2 \dot{m}}{\partial t^2} \tag{12b}$$

and combining equations (12a) and (12b) to get mass flow through pipe which is as follow:

$$\frac{\partial^2 \dot{m}}{\partial t^2} - v_c^2 \frac{\partial^2 \dot{m}}{\partial x_l^2} + \frac{R_t}{\rho}\frac{\partial \dot{m}}{\partial t} = 0 \tag{13}$$

Above equation is a generalized wave equation with an additional dissipative term. The proposed mass flow equation can be solved by using the following form (see [22]):

$$\dot{m}(x_l, t) = \chi(t)\Gamma(x_l, t) \tag{14}$$

Now, by introducing equation (14) into equation (13), the following equation is obtained

$$\ddot{\chi}(t)\Gamma(x_l,t)+2\dot{\chi}(t)\frac{\partial\Gamma(x_l,t)}{\partial t}+\chi(t)\frac{\partial^2\Gamma(x_l,t)}{\partial t^2}-v_c^2\chi(t)\frac{\partial^2\Gamma(x_l,t)}{\partial x_l^2}+\frac{R_t}{\rho}\dot{\chi}(t)\Gamma(x_l,t)+\frac{R_t}{\rho}\chi(t)\frac{\partial\Gamma(x_l,t)}{\partial t}=0 \tag{15}$$

and by rearranging above equation:

$$\left(\ddot{\chi}(t)+\frac{R_t}{\rho}\dot{\chi}(t)\right)\Gamma(x_l,t)+\left(2\dot{\chi}(t)+\frac{R_t}{\rho}\chi(t)\right)\frac{\partial\Gamma(x_l,t)}{\partial t}+\chi(t)\frac{\partial^2\Gamma(x_l,t)}{\partial t^2}-v_c^2\chi(t)\frac{\partial^2\Gamma(x_l,t)}{\partial x_l^2}=0 \tag{16}$$

In order to obtain implicit solution of the equation for $\Gamma(x_l,t)$, first $\chi(t)$ is determined such that, after substitution in equation (16), the remaining equation in $\Gamma(x_l,t)$ contains no term related to $\chi(t)$,

$$2\dot{\chi}(t)+\frac{R_t}{\rho}\chi(t)=0\ ,\quad \chi(0)\neq 0 \tag{17}$$

The analytical solution of equation (17) is given by:

$$\chi(t)=\chi(0)e^{-\frac{R_tRT_s}{2p_s}t} \tag{18}$$

and substituting the solution provided by equation (18) into (16)

$$\chi(0)e^{-\frac{R_tRT_s}{2p_s}t}\left[\frac{R_t^2R^2T_s^2}{4p_s^2}\Gamma(x_l,t)-\frac{R_t^2R^2T_s^2}{2p_s^2}\Gamma(x_l,t)+\frac{\partial^2\Gamma(x_l,t)}{\partial t^2}-v_c^2\frac{\partial^2\Gamma(x_l,t)}{\partial x_l^2}\right]=0 \tag{19}$$

subsequently, the solution of equation (19) is given by

$$\frac{-R_t^2R^2T_s^2}{4p_s^2}\Gamma(x_l,t)+\frac{\partial^2\Gamma(x_l,t)}{\partial t^2}-v_c^2\frac{\partial^2\Gamma(x_l,t)}{\partial x_l^2}=0 \tag{20}$$

which is a dispersive wave equation in 1D. It can be noticed that the tubes under consideration are very short, so the dispersion caused by the factor $\frac{-R_t^2R^2T_s^2}{4p_s^2}$ is assumed to be very small, and hence can be neglected, consequently:

$$\frac{\partial^2\Gamma(x_l,t)}{\partial t^2}-v_c^2\frac{\partial^2\Gamma(x_l,t)}{\partial x_l^2}=0 \tag{21}$$

It is assumed that there is no air flow through the tube at $t=0$, the flow at the inlet $(x_l=0)$ is a time dependent function $\dot{m}_{s-in}$ and there is no reflection from the end, connected at

the ITP. Solution of the non dispersive wave equation (21) with initial boundary problem is given by [20]:

$$\Gamma(x_l, t) = \begin{cases} 0 & , \quad t < x_l/v_c \\ \dot{m}_{s-in} & , \quad t \geq x_l/v_c \end{cases} \tag{22}$$

The input wave will reach the end of the tube in a time period $T = L_l/v_c$. Where L_l is length of the tube. Replacing t by L_l/v_c in equation (18), the mass flow at the outlet of the tube $x_l = L_l$ is,

$$\dot{m}(L_l, t) = \begin{cases} 0 & , \quad t < L_l/v_c \\ \Gamma(x_l, t)\chi(0)e^{-\frac{R_t R T_s}{2p_s}\frac{L_l}{v_c}} & , \quad t \geq L_l/v_c \end{cases} \tag{23}$$

The tube resistance R_t can be obtained from the expression for the pressure drop along the tube [22]:

$$\Delta p = f\frac{L_l \rho v_a^2}{2D} = R_t v_a L_l \tag{24}$$

where f is the friction factor and D is the inner diameter of the tube. As the flow is turbulent, friction factor f can be computed using the Blasius formula $f = \dfrac{0.316}{R_e^{1/4}}$. Here R_e is the Reynolds number and its value is grater than 4000 for turbulent flow. The tube resistance for turbulent flow is given by

$$R_t = 0.158\frac{\mu}{D^2}R_e^{3/4} \tag{25}$$

where μ is dynamic viscosity of the air. Total mass flow to the actuator is the difference of air mass flowing out from the actuator to reservoir and air mass flowing toward the actuator from atmosphere through pneumatic line

$$\dot{m}_s(x_l, t) = \dot{m}_{s-in}\chi_{in}(x_l, t) - \dot{m}_{s-out}\chi_{out}(x_l, t) \tag{26}$$

2.2.2 Volume of the pocket

To design an active inflatable system, two types of ITPs can be used i.e. elliptical and spherical shaped pockets. Both ITPs are shown in Fig. 4 along with figure showing their three dimensions. It has been observed that the air leakage problem inside the ITPs of spherical and elliptical shapes is lesser than other types. Therefore both these types are

used for further analysis [8]. The volume of the pocket V_s varies with the amount of air inside it. Consequently, it is modelled and identified as a function of pressure.

Figure 4: Inflatable Textile Pockets (ITP) with their three dimensional view (spherical and elliptical shaped)

Next, the variation in volume is studied for both shapes by considering the elastic deformation of the material. Firstly, an elliptical geometry of pocket (air bag) has been considered. The obtained model is then modified to investigated a spherical shape.

Elliptical shape

According to the theory of pressure vessels [17, 23], the hoop stress σ_θ and the longitudinal stress σ_a can be obtained using the following equations:

$$\sigma_a = \frac{a_{in}\,(p_s - p_{atm})}{2sc_{in}}\ ,\ \ \sigma_\theta = \frac{a_{in}\,(p_s - p_{atm})}{2sb_{in}^2}\frac{2b_{in}^2 - c_{in}^2}{c_{in}} \tag{27}$$

where s is the thickness of the fabric material. Here a_{in}, b_{in} and c_{in} are the initial dimensions of elliptical shaped pocket. The knowledge of the stresses allows to calculate the elastic deformations and, consequently, variation in the dimensions of the pocket. The elastic deformations ε_a and ε_θ can be expressed in terms of material characteristics as follows [17]:

$$\varepsilon_a = \frac{1}{E}\left(\sigma_a - \nu\sigma_\theta\right)\ ,\ \ \varepsilon_\theta = \frac{1}{E}\left(\sigma_\theta - \nu\sigma_a\right) \tag{28}$$

where E and ν are the Young modulus and the Poisson's ratio of the fabric material.

$$\varepsilon = \frac{\Delta l}{l} = \frac{l_{fin} - l_{in}}{l_{in}} \tag{29}$$

Therefore, the values of final dimensions of the elliptical pocket can be expressed using

the following equations:

$$a_{fin} = a_{in}\,(1+\varepsilon)\ ,\ b_{fin} = b_{in}\,(1+\varepsilon)\ ,\ c_{fin} = c_{in}\,(1+\varepsilon) \tag{30}$$

where a_{fin}, b_{fin} and c_{fin} represent the final dimensions of elliptical shaped pocket. So, the equation for the variation in volume is given by [23]:

$$\dot{V}_s = V_{fin} - V_{in} = \frac{4}{3}\pi\left(a_{fin}b_{fin}c_{fin} - a_{in}b_{in}c_{in}\right) \tag{31}$$

Note: Due to the symmetry in the spherical shaped pocket, both stresses are equal i.e. $\sigma_a = \sigma_\theta = \sigma$. Therefore, the variation in the volume of the spherical shaped pocket can also be obtained by using generalized equation (31) of the ellipse [23]:

$$\dot{V}_s = V_{fin} - V_{in} = \frac{4}{3}\pi\left(r_{fin}^3 - r_{in}^3\right) \tag{32}$$

where r_{in} and r_{fin} are the initial and final values of the radius of the sphere.

2.2.3 Inflatable Textile Pocket (ITP) model

The inflatable textile pocket can be modelled as an equivalent mechanical system whose rigidity and damping depend on the pressure inside it. Therefore, it may be represented via spring and damper system which counteract the applied external force. In a first approach, all the external forces acting on the surface of the hemisphere (ITP) are represented by an equivalent normal force F_{ext}. Different forces involved in the system are shown in Fig. 5.

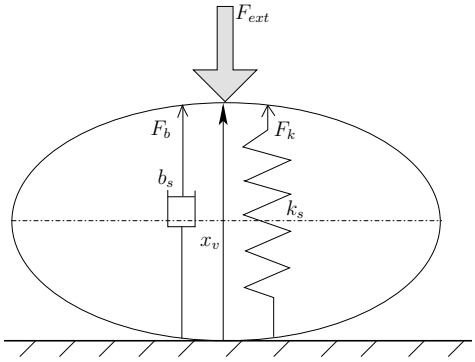

Figure 5: Equivalent diagram of an ITP with all important forces acting on it

The equivalent mechanical system can be modelled as a mass-spring-damper system under the effect of equivalent external force due to pressure difference across the ITP. Using Newton's second law of motion, it can be expressed as:

$$m_v \ddot{x}_v = F_{ext} - d_s \dot{x}_v - k_s x_v \tag{33}$$

where m_v, x_v and F_{ext} are, respectively, the pocket mass, its vertical position and the external force acting on it. The terms k_s and d_s represent the spring and the damping coefficients due to the deformation of the inflatable pocket. As rigidity and damping of the pocket depend on pressure, the coefficients of ITP model are identified as a function of pressure inside it.

2.3 Generalized model of the active inflatable device

Finally, a generalized model of an inflatable device is obtained by combining all sub-models, as shown in Fig. 6.

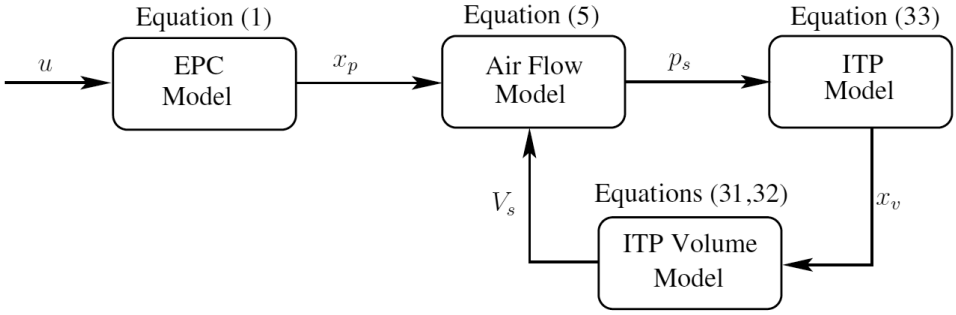

Figure 6: Diagram showing inputs and outputs of each subpart of the system

The proposed ITP model is represented in the state space form:

$$\begin{aligned}
\dot{x}_1 &= x_2 \\
\dot{x}_2 &= \left(F_{mag} - \left(x_5 - p_{atm}\right) A_p - d_p x_2 - k_p x_1\right) / m_p \\
\dot{x}_3 &= x_4 \\
\dot{x}_4 &= \left(F_{ext} - d_s(x_5)\, x_4 - k_s(x_5)\, x_3\right) / m_v \\
\dot{x}_5 &= \frac{\sqrt{\gamma R T_s}}{V_s} A_{eff} \left[\chi_{in} \frac{x_5}{\sqrt{T_s}} \Phi\left(p_r\right) - \chi_{out} \frac{p_{res}}{\sqrt{T_{res}}} \Phi\left(p_r^*\right)\right] - \frac{4\pi a b x_4}{3 V_s} x_5
\end{aligned} \tag{34}$$

where x_1, x_2, x_3, x_4 and x_5 are, respectively, the state variables for the spool valve position and its velocity, the vertical position of the pocket, its velocity and the pressure inside the pocket chamber. In equation (34) it is supposed that for both elliptical and spherical shaped ITPs, two dimensions remain the same after pressurizing the pockets. Therefore, it is considered that $a_{in} = a_{fin} = a$ and $b_{in} = b_{fin} = b$ in equation (31). Similarly, for the round shaped ITP it is considered that $r_{in} = r_{fin} = r$ in two directions, only, i.e. x and y in equation (32); which gives a generalized form of the model in (34). The model can be easily adapted to take the other sub-models into consideration, which ensures the flexibility in the derived model.

3 Parameter identification of the active inflatable device

The parameter identification of the active inflatable device model from experimental measurements is presented in this section. The parameter identification process is carried out by decomposing the whole model into sub-systems. In this way, a complex identification problem is transformed into relatively simple identification models. At the end, the solution of the whole identification problem is provided by taking into account judiciously the solution of each sub-problem. The experimental measurements are obtained with the help of two specific test benches. One test bench has been used and other one has been developed to validate the oriented modelling of two types of inflatable pocket (spherical and elliptical shaped).

3.1 Employed test benches

Firstly, a servo-hydraulic fatigue testing machine INSTRON 8801 (see Fig. 7) is used to study the characteristics of the two spherical and elliptical shaped ITPs. This machine allows to apply both the static and dynamic external forces up to 50 KN on an object with a good accuracy and precision. The force and position sensors information are acquired with Dspace® board for further identification and validation. This analysis helped in identifying the pressure dependent spring and damping coefficients of both pockets.

A second test bench has been developed in order to verify the modelling approach with

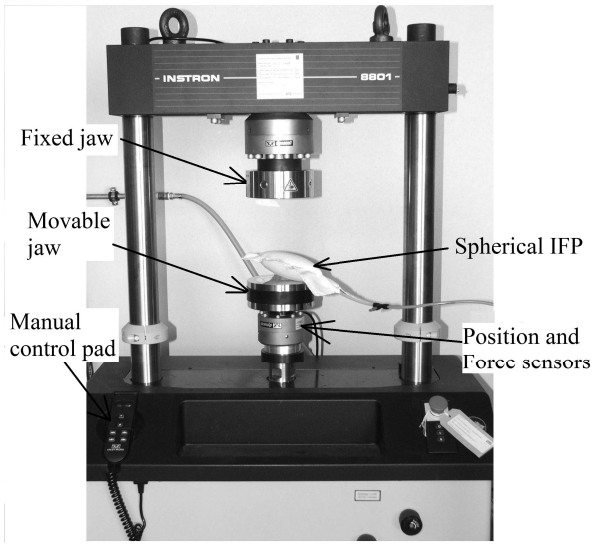

Figure 7: Test bench for fatigue testing (INSTRON 8801)

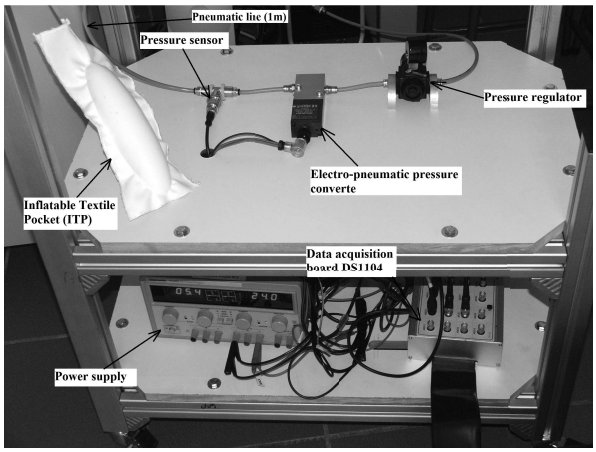

Figure 8: Test bench for the validation step of the developed model

the whole system in real conditions. The developed experimental test bench consists of a power supply, a pressure converter, a pressure sensor, an ITP and a data acquisition system (a Dspace® DS1104 controller board). The pressure regulator is a proportional valve Festo MPYE-5-M5-010-B which works with the controlled voltage applied through Dspace® board and it varies from 0 to 10V. The pressure source, applied to the system, is regulated via a manual pressure regulator. Fig. 8 shows the complete experimental test bench.

3.2 Identification of EPC parameters

The EPC system, as described in section 2.1, is a solenoid based linear actuator which contains a spring to bring the solenoid back to its original position. To identify the parameters of the EPC, the later is represented as a transfer function of second order system (35) using (1) and (2).

$$T_s = \frac{X_p}{U} = \frac{De^{-s\tau} + (p_s - p_{atm})A_p/U}{m_p s^2 + d_p s + k_p} \tag{35}$$

The term D represents the gain of the transfer function, as $D >> (p_s - p_{atm})A_p/U$. By applying off-line identification procedure with least square method, all parameters of the EPC can be identified. These parameters are provided in Table 1.

Table 1: Parameters values for the EPC and the ITP used for simulation

Parameter	Value	Parameter	Value
A_p	$7.07\,10^{-4}m^2$	R	$287Jkg^{-1}K^{-1}$
m_p	$0.152kg$	T_s	$293K$
d_p	$25.78Nsm^{-1}$	m_v	$0.1kg$
k_p	$1000Nm^{-1}$	b_{in}	$0.155m$
D	$0.64Nvolt^{-1}$	c_{in}	$0.045m$
γ	1.4	r_{in}	$0.075m$
s	$2\,10^{-3}$	E	$1\,10^{8}Nm^{-2}$
ν	0.3	p_{atm}	$9.875\,10^{4}Pa$

3.3 Identification of ITP parameters

As seen in the developed model, certain parameters of the model need to be identified to validate the complete model of the system. The dynamics of the pressure converter are difficult to model as it comes with a built-in electronic system, which renders the delay in control signal and air leakage around mid position of spool valve. Therefore, these two phenomena are considered by using the static maps of delay and leakage pressure. The other identified parameters are the effective flow area A_{eff}, the spring coefficient k_s and the damping coefficient d_s of the Inflatable Textile Pocket.

3.3.1 Affective flow area A_{eff}

The air flow area through the pressure regulator is obtained as a function of plunger position. It is required to determine the air mass flow entering or leaving the actuator chamber. The dynamics of pressure inside ITP with high bandwidth sensor are used to identify the flow area. From equation (5), air mass flow rate can be determined after assuming that the temperature of the actuator chamber remains constant. With measured actuator pressure, movable jaw position of INSTRON 8801, reservoir pressure, atmospheric pressure and air mass flow, the effective flow area between atmosphere and actuator or between actuator and reservoir can be obtained by using the equations (5), (6) and (9). Then,

$$A_{eff} = \left[\frac{\dot{p}_s V_s}{RT_s} - \frac{p_s V_s}{RT_s}\dot{V}_s\right] \sqrt{\frac{T_0}{R}} / \left(p_0 \Phi\left(p_r\right)\right) \tag{36}$$

where T_0 and p_0 are the upstream temperature and pressure. Fig. 9 shows the effective flow area as a function of the applied voltage signal for the Festo MPYE-5-M5-010-B electro-pneumatic pressure converter.

3.3.2 Spring and damping coefficients

As described in previous section, tests were performed with INSTRON test bench on two different types of ITPs. To identify the spring and damping coefficients, different steps of pressure inside each pocket are applied. The compression of the pocket is measured with a position sensor integrated in the INSTRON 8801. The ratio of applied force and pocket displacement will give the value of spring coefficient at each pressure.

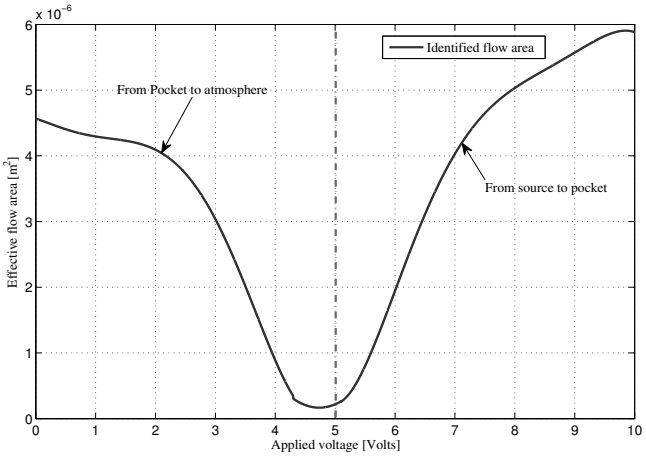

Figure 9: Effective flow area vs applied voltage

The spring coefficients are identified from least square method, as a function of pressure inside pockets. Finally, the obtained polynomials are given below:

$$k_s(Sphere) = -13889p_s^2 + 13270p_s + 46.76 \tag{37a}$$

$$k_s(Ellipse) = -9522.5p_s^2 + 15620p_s - 42.9 \tag{37b}$$

Fig. 10 shows identified spring coefficients at different pressures for both the elliptical and spherical shaped pockets.

The air inside the pocket makes it a spring-damping system which is equivalent to a second order system whose transfer function is obtained from the equation (33):

$$T_s = \frac{F_{ext}}{X_v} = \frac{1}{m_v s^2 + d_s s + k_s} \tag{38}$$

By applying the least square method for off-line identification at constant pressure inside ITP, the damping coefficients for both types of ITPs are obtained. The final identified polynomial functions for the variation in damping coefficients for both the pockets are given below:

$$d_s(Sphere) = -1527.4p_s^4 + 2196p_s^3 - 1097.7p_s^2 + 241.7p_s + 0.064 \tag{39a}$$

$$d_s(Ellipse) = -2130p_s^4 + 2648.4p_s^3 - 1198.6p_s^2 + 264.3p_s + 0.118 \tag{39b}$$

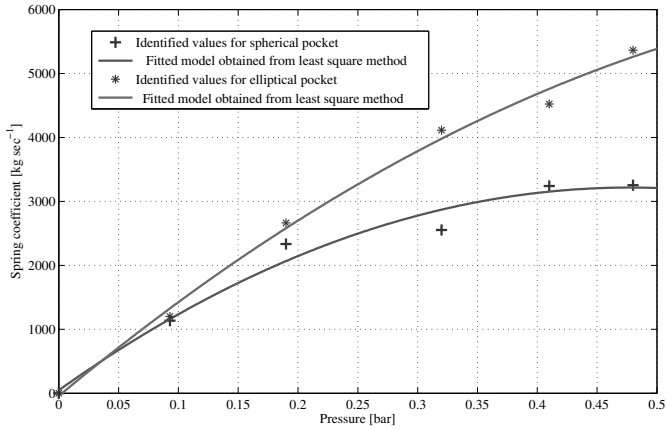

Figure 10: Identified spring coefficient for both spherical and elliptical shaped pockets

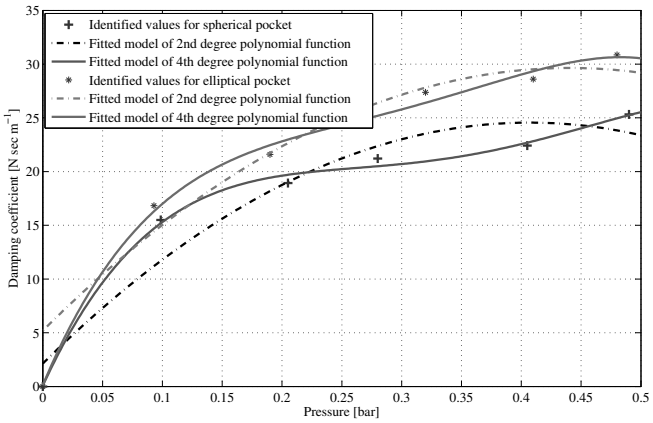

Figure 11: Identified damping coefficients for both spherical and elliptical shaped pockets

Fig. 11 shows the identified damping coefficients as a function of pressure inside pocket. whereas, the remaining identified parameters are provided in Table 1.

3.3.3 Air leakage

The spool of pressure converter allows the air to pass through it. The point where it stops the passage of air is the middle point when the applied signal is 5V. Because at this point spool blocks the outlet port. However, this blockage shows dead zone area. Consequently,

this blockage causes the leakage of air in the pocket through EPC ports. Moreover, this leakage increases with the decrease in pocket volume. This phenomenon is quite difficult to characterize and to model. Therefore, in a first approach, a static map for leakage pressure was chosen in order to validate the whole model. In Fig. 12, the identified air leakage is shown for both the pockets.

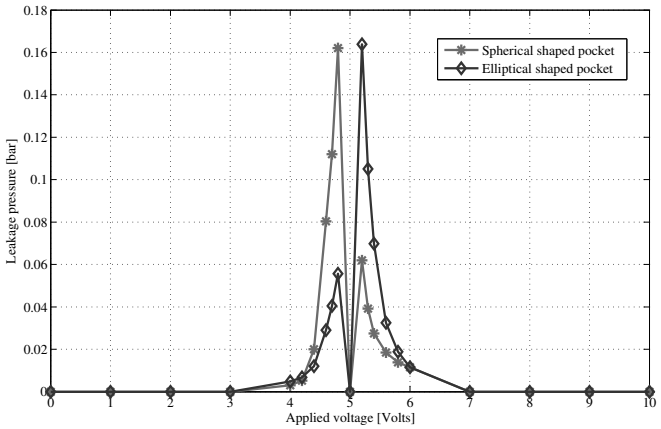

Figure 12: Pressure drop due to the air leakage through the valves of pressure regulator

Due to the air leakage at closed center and the positions near by, various pressure gains are obtained for step signals applied to both types of ITPs. These positions correspond to applied signals from 4V to 6V. Due to the air leakage, the down stream pressure due to this flow changes. Whereas, ideally the value of the pressure must remain constant. Hence, this phenomenon is expressed as:

$$p_{down} = p_{down}(ideal) - \delta p \tag{40}$$

where p_{down} is the down stream pressure for both the inward and outward flow directions and δp is the pressure lose due to leakage. The lookup table for air leakage is given in Table.2.

Table 2: Lookup table for the leakage pressure δp and time delay function τ

u (volts)	0.5	3.5	4	4.2	4.4	4.6	4.8	5	5.2	5.4	5.6	5.8	6	6.5	9.5
δp (bar)	0	0	-0.003	-0.0052	-0.02	-0.08	-0.16	0	0.062	0.027	0.018	0.014	0.011	0	0
τ (sec)	0.01	0.15	0.58	0.95	1.1	1.32	1.46	1.44	1.2	1	0.6	0.5	0.37	0.2	0.01

4 Active inflatable device model validation

The model obtained in the previous section with identified parameters given in Table.1 and Table.2 is validated, considering the following three sub-parts of the EPC based ITP system: 1) Volume of the pocket, 2) Pressure converter dynamics and 3) Strength of the ITP.

4.1 Volume of the pocket

First, the variation of the volume of the pocket is considered by using elastic deformation method (see Section 2.2.2).

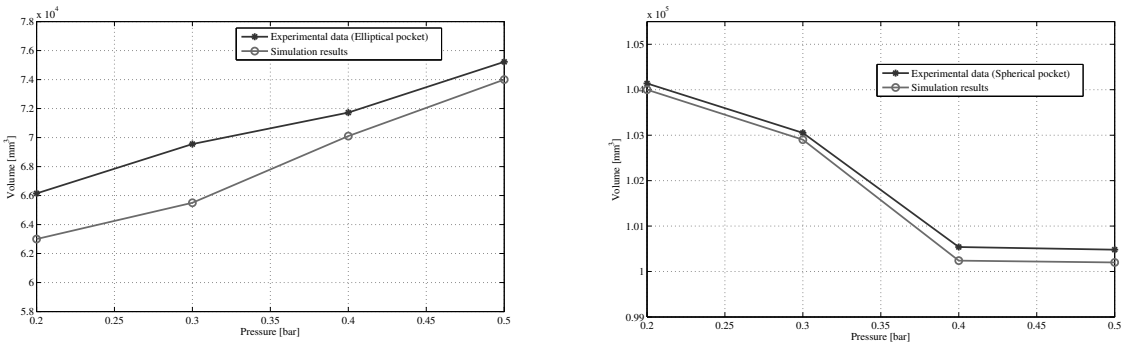

(a) Elliptical shaped

(b) Spherical shaped

Figure 13: Variation of the volume of the pocket as a function of pressure inside the pockets

Fig. 13 shows the comparison between the evolution of the volume as a function of pressure obtained experimentally and the results obtained by simulation. It is observed

that the volume of the spherical ITP decreases with increase in pressure. However, for the elliptical ITP, volume of the pocket increases, linearly, with increase of its rigidity caused by the pressure.

4.2 Pressure converter dynamics

The next part in the system is to validate the Electro-pneumatic Pressure Converter (EPC) dynamics which depends on the spool movement and the air mass flow. Input to the EPC is the applied voltage signal which varies from 0 to 10 V. When this signal is less than 5 V then air can flow from ITP to atmosphere and when it is greater than 5 V, it flows from pressure source to the ITP. At the closed centered i.e. 5 V, air flow is zero in both directions.

4.2.1 Step response

At first stage, the test bench shown in Fig. 8 is used, to validate the pressure dynamics inside the ITP. The identified effective flow area A_{eff} provided in Fig. 9 is used to determine air mass flow dynamics. The pressure dynamics inside an elliptical shaped pocket are shown in Fig. 14.

The lengths of major and minor axis are $15.5cm$ and $4.5cm$, respectively, for the ellipse and the radius of spherical pocket is $7.5cm$. The length of pneumatic tube line joining the EPC with the ITP is 1m long. The measured pressure dynamics are compared with simulation results obtained from the developed model. Results in figures 14(a), 14(b) and 14(c) show the comparison between experiments and simulation results obtained without using air leakage function. Whereas, Figs. 14(d), 14(e) and 14(f) show the results with air leakage function incorporated into the model. It can be seen that this non linear behaviour appears only near central position of the spool valve i.e. the position when applied voltage signal is between 4V and 6V. Fig. 15 shows the step response with a spherical shaped pocket. results are shown for three step input voltages. Where, figures 15(a), 15(b) and 15(c) show the comparison between experiments and simulation results obtained without using air leakage function and figures 15(d), 15(e) and 15(f) with air leakage function

incorporated into the model. Thus, the actuator model that incorporate the air leakage function gives closed results compared to measured ones.

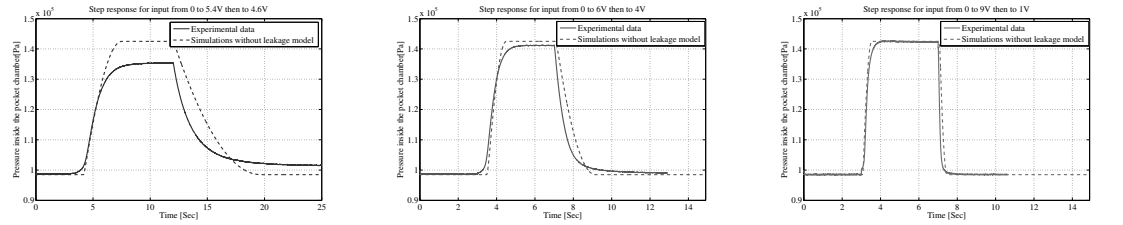

(a) without leakage function at 5.4V (b) without leakage function at 6V (c) without leakage function at 9V

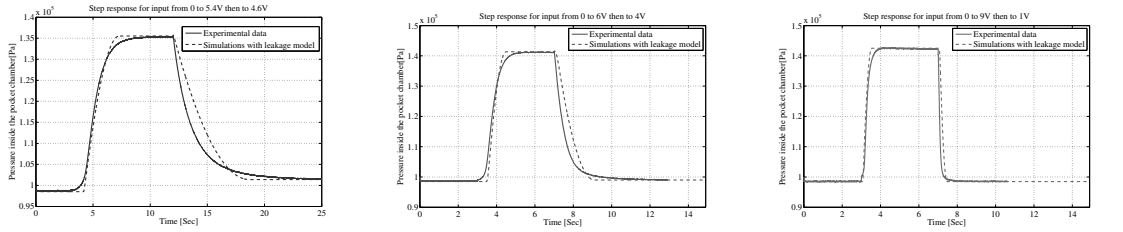

(d) with leakage function at 5.4V (e) with leakage function at 6V (f) with leakage function at 9V

Figure 14: Pressure inside elliptical shaped ITP for different step signals

4.2.2 Sinusoidal response

Similarly, the pressure dynamics inside on both ITPs are validated considering as reference signal a low frequency sine voltage function of $0.15Hz$ with amplitude of 8V (1V to 9V). The experimental and simulation results for both types of pocket are shown in Fig. 16. As can be seen, the identified model shows closed response as compared to measured ones.

4.3 ITP dynamics

Last part of model validation is carried out on a servo hydraulic machine INSTRON 8801. This setup allows us to study the strength of an ITP. In these tests, the pressure inside a pocket is kept constant and an external force is applied through INSTRON 8801 to analyse the pocket compression with respect to force. These tests are repeated at different gauge

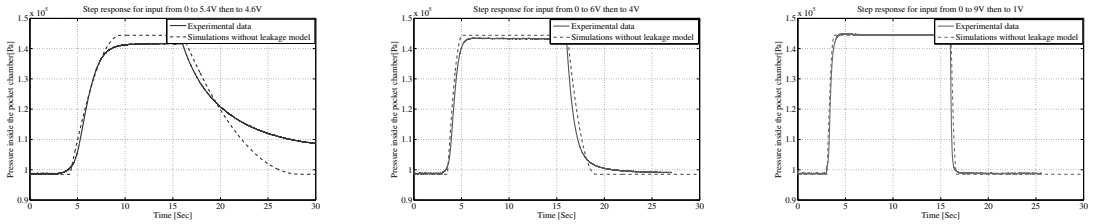

(a) without leakage function at 5.4V (b) without leakage function at 6V (c) without leakage function at 9V

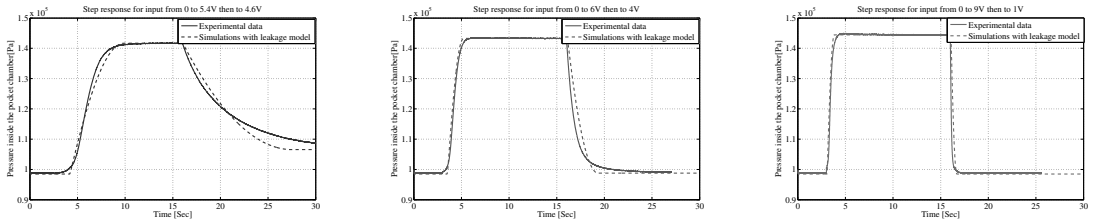

(d) with leakage function at 5.4V (e) with leakage function at 6V (f) with leakage function at 9V

Figure 15: Pressure inside spherical shaped ITP for different step signals

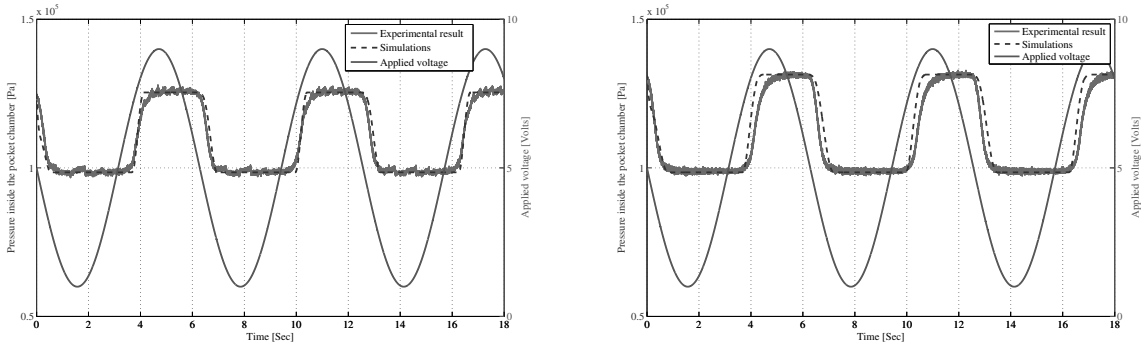

(a) Elliptical shaped pocket (b) Spherical shaped pocket

Figure 16: Pressure inside the pockets for reference sine signal of $0.15Hz$

pressures ranging from 0.2 to 0.5 bar for a given external force of both step and sine wave forms.

4.3.1 Step response

Fig. 17 shows the step response (pocket displacement) for $20N$ input force at different prefixed internal pressures. These simulation and experimental results are shown for both types of pocket. As the internal pressure inside the ITP is increased, the stiffness increases as well and the pocket displacement decreases under the sine input force.

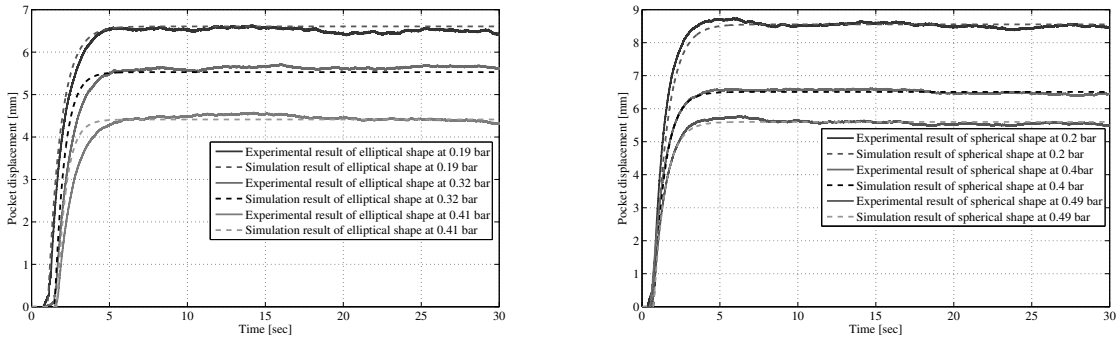

(a) Elliptical shaped pocket

(b) Spherical shaped pocket

Figure 17: Step responses for the applied force on the pocket at different pressure values inside it

4.3.2 Sinusoidal response

In a second test, the model is validated for an applied force on the ITP with a shape of sine wave. Due to the limitation in the INSTRON machine, the tests are performed only at low frequencies, here $0.1Hz$. Fig. 18 shows test bench results for both elliptical shaped and spherical shaped pockets. Just like the previous case, the increase of the internal pressure inside the pocket implies the increase of the stiffness of the system and, therefore, the displacement decreases for the same applied force.

The performance of the proposed model can be evaluated using the Mean Square Error (MSE) and the Variance-Accounted- For (VAF) indicators as described in [24]:

$$MSE = \frac{1}{n}\sum_{i=1}^{n}\left(y_a(i) - y(i)\right)^2 \tag{41}$$

$$VAF = \max\left[1 - \frac{var(y_a(i) - y(i))}{var(y_a(i))}, 0\right] \times 100 \tag{42}$$

where $y_a(i)$ and $y(i)$ are the actual and model output, n represents the number of data points and the function var describes the variance of the output. The performance indicators obtained for the nonlinear model are $MSE = 0.0381$ and $VAF = 98.139\%$ using the responses to the applied sine force at low frequency of $0.1Hz$. These indices show the effectiveness of the proposed model.

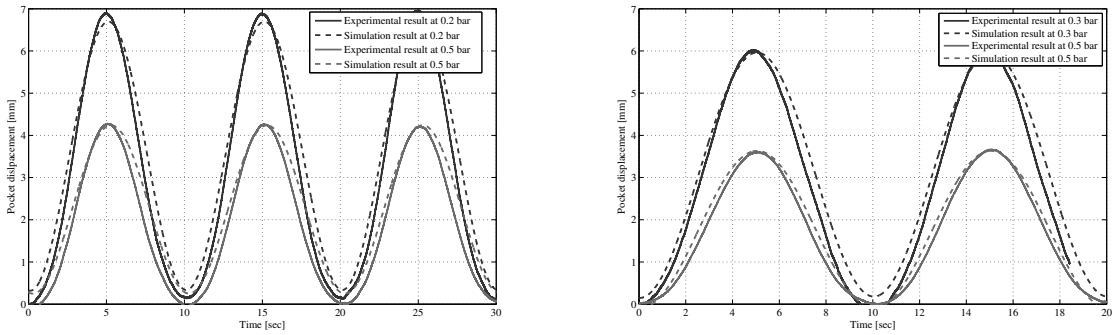

(a) Elliptical shaped pocket

(b) Spherical shaped pocket

Figure 18: Responses to the applied sine force at low frequency of $0.1Hz$, on the pocket for different constant pressures inside it

5 Conclusions

A structured mathematical model of an active inflatable device is proposed in this article. The proposed device is composed of Inflatable Textile Pocket (ITP), with spherical and elliptical shapes. The whole system consists of a pressure source, a pressure regulator and an ITP. Pressure regulator dynamics are studied to obtain a calibrated model, with the help of a new developed test benches. Validation tests show good results and confirm the effectiveness of the proposed mathematical model, for both static and low dynamics of pressure variations as well as external forces. Future perspectives of the work are model based control design of the pressure inside the pocket, by considering different criteria and to integrate these pockets in a complex inflatable device using several ITPs.

Acknowledgments

This work is sponsored by the regional project ERGOFLUX [CONECTUS-OSEO]. Furthermore, the authors are grateful to Robin PRUD'HOMME, Alicia GAURIVAUD undergraduate students of ENSISA-UHA and Gina SALUCCI from the University of Salerno , for their support.

References

[1] A. Chawla, P. V. Bhosale, and S. Mukherjee. Modeling of folding of passenger side airbag mesh. *SAE technical paper*, (2005-26-059), 2005.

[2] D. G. Rangnath. Modeling and analysis of an inflatable lap belt airbag restraint system for frontal crash protection of mass transit bus operators. *Masters thesis, Wichita State University, USA*, 2009.

[3] T. M. Seigler. A comparative analysis of air-inflated and foam seat cushions for truck seats. *Masters thesis, Virginia Polytechnic Institute and State University, USA*, 2002.

[4] L. V. Langenhove and C. Hertleer. Smart textiles in vehicles: A foresight. *Journal of textile and apparel technology and management*, 3(4):1–5, 2004.

[5] A. Rasheed, J. Y. Drean, A. Sinoimeri, and A. Shafi. Capteur de pression flexible. *French patent no. 1259578*, 2012.

[6] M. A. Tulemat. Etude de poches tissees complexes gonflables: Application automobile. *PhD thesis (French), Université de Haute-Alsace, France*, 2007.

[7] B. K. Behera and R. Mishra. 3 dimensional weaving. *Indian Journal of Fibre and Textile Research*, 33:274–287, 2008.

[8] M. Alali. Conception d'une machine de fatigue: test de poches complexes tissèes (french). *Masters thesis, Université de Haute-Alsace, France*, 2008.

[9] Z. Rao and G.M. Bone. Nonlinear modeling and control of servo pneumatic actuators. *IEEE Transactions on Control Systems Technology*, 16(3):562–569, 2008.

[10] K. C. Wickramatunge and T. Leephakpreeda. Empirical modeling of dynamic behaviors of pneumatic artificial muscle actuators. *ISA Transactions, In press*, 52(6):825–834, 2013.

[11] N. Gulati and E. J. Barth. Dynamic modeling of a monopropellant-based chemofluidic actuation system. *Journal of dynamic systems measurement and control*, 129:435–445, 2007.

[12] O. Olaby, X. Brun, S. Sesmat, T. Redarce, and E. Bideaux. Characterization and modeling of a proportional valve for control synthesis. *In Proc. 6th JFPS symposium on Fluid Power, Tsukuba, Japan*, 2005.

[13] T. Zilic, D. Pavkovic, and D. Zorc. Modeling and control of a pneumatically actuated inverted pendulum. *ISA Transactions*, 48:327–335, 2009.

[14] J. Zhang, C. Lv, X. Yue, Y. Li, and Y. Yuan. Study on a linear relationship between limited pressure difference and coil current of on/off valve and its influential factors. *ISA Transactions, In press*, 53(1):150–161, 2014.

[15] J. Heywood. *Internal Combustion Engine Fundamentals*. Publishers McGraw-Hill, ISBN-13: 978-0070286375, 1988.

[16] A. Mehmood. Modeling, simulation and robust control of an electro-pneumatic actuator for a variable geometry turbocharger. *PhD thesis, Université de Technologie de Belfort-Montbeliard, France*, 2012.

[17] D. W. Lee. An innovative inflatable morphing body structure for crashworthiness of military and commercial vehicles. *PhD thesis, University of Michigan, USA*, 2008.

[18] P.W. Lim, N.C Cheung, and M.F. Rahman. Proportional control of a solenoid actuator. *20th International Conference on Industrial Electronics, Control and Instrumentation*, 3:2045–2050, 1994.

[19] P.H. Oosthuizen and W. Carscallen. *Compressible Fluid Flow*. Publishers McGraw-Hill, ISBN-13: 978-0070481978, 1997.

[20] B. W. Andersen. *The Analysis and Design of Pneumatic Systems*. Krieger Pub Co. (revised edition), ISBN-13: 978-1575241647, 2001.

[21] C. B. Schuder and R. C. Binder. The response of pneumatic transmission lines to step inputs. *ASME Journal of Basic Engineering*, 81:578–584, 1959.

[22] E. Richer and Y. Hurmuzlu. A high performance pneumatic force actuator system: Part 1 - nonlinear mathematical model. *Journal of dynamic systems, measurement and control*, 122:416–425, 2000.

[23] D. M. Fryer and J. F. Harvey. *High pressure vassels*. Publishers Chapman and Hall, ISBN-13: 978-0412074516, 1998.

[24] R. Orjuela, B. Marx, J. Ragot, and D. Maquinc. Nonlinear system identification using heterogeneous multiple models. *International Journal of Applied Mathematics and Computer Science*, 23(1):103–115, 2013.